

Effects of Nickel Oxide Nanoparticles on Visual Processes and Electro-Retinography Waves in the Bullfrog Eye

¹Fazli Wahid*, ¹Romana Khan, ²Taous Khan, ³Mazhar Ul-Islam, and ⁴You Young Kim**

¹Department of Environmental Sciences, COMSATS Institute of Information Technology, 22060, Abbottabad, Pakistan.

²Department of Pharmacy, COMSATS Institute of Information Technology, 22060, Abbottabad, Pakistan.

³Department of Chemical Engineering, Dhofar University, Salalah, 211, Sultanate of Oman.

⁴School of Life Sciences and Biotechnology, College of Natural Sciences, Kyungpook National University, Daegu 702-701, South Korea.

fazliwahid@ciit.net.pk*, yykim@knu.ac.kr**

(Received on 12th March 2015, accepted in revised form 6th October 2015)

Summary: The nickel oxide nanoparticles were synthesized and their effects were evaluated on the visual system of the vertebrate eye. The physico-chemical characterization of the prepared nanoparticles was carried out through transmission electron microscopy (TEM) and X-ray diffraction (XRD) measurements. Electroretinography (ERG) was used to evaluate the possible effects of the nickel oxide nanoparticles on the visual system. TEM and XRD measurements demonstrated that the size of nickel oxide nanoparticles was in the range of 4-10 nm. ERG results showed that nickel oxide nanoparticles markedly improve ERG b-wave amplitude during dark-adapted and in the presence of background light. Nickel oxide nanoparticles increased visual sensitivity by 0.4 log units of light intensity and also shortened the time required for rhodopsin regeneration. In conclusion, nickel oxide nanoparticles have positive effects on visual processes in vertebrate eye.

Keywords: Nickel oxide nanoparticles; Electroretinography; Visual sensitivity; Nanomedicine; Eye; Retina

Introduction

Nanomaterials are very small scale particles between 1 and 100 nm in size [1]. These are comparable to biomolecules, which are capable of crossing the cell membrane to reach into the cell interior where they may interact with intracellular molecules [2]. Based on this property, extensive research has been carried out on the possible medical applications of nanomaterials [3, 4]. In this regard, nanomaterials have anti-cancer, anti-bacterial, and anti-viral activities [5-7]. More organized research was carried out in the last decade to screen nanoparticles for use in industrial, pharmaceutical, and medical fields [1-4].

The nickel oxide nanoparticles (NiONP) have diverse applications including uses in electrochromics preparation, making of films, p-type transparent conducting films, and synthesis of magnetic materials, gas sensors, catalysts, battery cathodes, and solid oxide fuel cell anodes [8]. Moreover, Ni and NiO core/shell nanoparticles have also been studied for the particular binding and as a magnetic separator of histidine-tagged proteins [9].

Electroretinography (ERG) is a common tool to measure the collective electrical responses of the retina after photostimulation [10, 11]. This technique has clinical applications for the detection of retina malfunctions and eye diseases [12].

Similarly, ERG has been extensively used in eye research to obtain information about visual functions that are not easily available through other means [12]. Generally, a representative ERG has four different regions: a-, b-, c-, and d- waves. Each wave represents the activity of specific kinds of cells [13-16]. The stimulation of photoreceptors generates ERG a-waves. The activity of bipolar and Muller cells produces the ERG b-wave [13-16]. The retinal pigment epithelium (RPE) produces the ERG c-wave, while the OFF bipolar and/or horizontal cells are responsible for the ERG d-wave [15, 17]. The ERG b-wave is very important, sensitive, and easy to record. Most importantly, ERG b-waves are associated with the assessment of visual sensitivity and eyesight [10, 11].

NiONP have recently received the attention of many researchers for their medical applications but have rarely been investigated in eye research. Therefore, the current study was carried out to determine the effects of NiONP on the visual functions of the vertebrate eye including visual processes, ERG b-waves, and rhodopsin regeneration using ERG techniques. NiONP treatment was found to augment the ERG b-wave, increase visual sensitivity, and shorten the duration for rhodopsin regeneration. These results may lay the foundation

*To whom all correspondence should be addressed.

for biomedical applications of NiONP and other related nanomaterials in eye research.

Experimental

Chemicals

All chemicals used in this study were of analytical grade. The chemicals used in preparation of Ringer's solution and in synthesis of NiONP were obtained from Sigma-Aldrich (St. Louis, MO, USA).

Synthesis of NiONP

The synthesis of NiONP was carried out through the method described by Dharmaraj *et al* [18]. Briefly, Ni(OAc)₂·4H₂O (0.1 mol) was mixed with 2-methoxy ethanol (1 mol) at 60°C for 2 h with continuous stirring. A solution of PVAc (14% wt./v) was prepared in DMF. In next step, nickel acetate and PVAc solutions were mixed in 1:4 ratios and stirred continuously for 3 h at room temperature to obtain a homogenous composite mixture. The prepared mixture was heated up to 150°C to remove the solvent and water. After this, the solid residue was powdered and calcined at 450°C to obtain the NiONP.

Characterization of NiONP

The size and structure of NiONP were analyzed through transmission electron microscopy (TEM). The nanoparticles were thoroughly dispersed in ethanol by sonication and spread on a copper grid. The analyses were carried out on Hitachi H7600 (HITACHI, LTD) TEM with digital and film cameras. The accelerating voltage of the instrument was 100 kV. The average particle size was calculated from TEM results using ImageJ software. The XRD analysis of the NiONP was carried out on an X-Ray Diffractometer (X'Pert-APD Phillips, Netherlands). The machine had an X-ray generator (3 kW) and anode (LFF Cu). The produced radiation was Cu K α of 1.54 Å wavelengths. The X-ray generator was set at 40 kV tension and 30 mA current. The angle of scanning was 10–70°. The average crystallite size was calculated from the XRD results using the Scherrer's formula.

Experimental Animal

To study the effects of NiONP on visual processes, bullfrogs (*Rana castesbeiana*) were used as model animals because the instrumentation was specifically designed for this animal. As it was not possible to perform the experiment on diseased eyes,

all experiments were conducted on normal eyes. The animals were supplied by a local dealer in Daegu (South Korea), kept and treated according to institutional (Kyungpook National University, South Korea) committee guidelines that are in total agreement with international recommendations for use and care of experimental animals (NIH Guide for the Care and Use of Laboratory Animals, NIH publication No. 85-23, 1985).

Animal Preparations and Dissection

The animals were dark adapted for at least 1 h before experimentation. The bullfrogs were then slaughtered and as soon as possible both the eyes were enucleated. The hemi-sect eyeball was incised, the internal part discarded, and the remaining parts (containing the retina) were mounted on a sample holder. The mounted eye was fixed in a modified Ussing chamber permanently located in a Faraday cage. The sample holder was perfused with basic Ringer's solution with constant oxygen supply. In order to avoid retinal damage all these steps were performed at room temperature under dim red light. The mounted eye was left uninterrupted (20-30 min) till a stable base line and reproducible ERG recordings were achieved. Subsequent to stabilization, control ERG recording were made for all range of light intensities. As soon as control recordings were completed, the same eyecup was treated with NiONP using calculated concentrations. After 20-30 min of NiONP treatments, ERG were recorded for all range of light intensities and compared with control readings. NiONP were suspended in Ringer's solution and thoroughly mixed with vortexing before each treatment. For this study, the NiONP stock solution was made as 0.1 g/ml whereas the final concentration was used as 200µg/ml. Each side of the Ussing chamber had a capacity of 15 ml ringer solution so the calculation for the final concentration was made accordingly.

Stimulation

The ERG chamber was equipped with a computer-controlled stimulus and background illumination source (12V/100V, halogen lamp). The stimulus light source was set to deliver 505 nm monochromatic light. The flash duration was constant and fixed at 200 ms for all the experiments. The background light source supplied the same monochromatic light for a long duration. Calibrated neutral-density and interference filters were used in all protocols in order to control the intensity and color of the flashes. The stimulation of the eyecup was started with low intensity and then gradually

amplified by 0.5 log steps. For the restoration of eyecup sensitivity, sufficient time (1-4 min) was given between two stimulations. The un-attenuated stimulus flash intensity was 2.48 cd s/m² (candela x seconds/meters squared) while the transported was 1.95×10¹⁴ photons/cm²/sec. The background illumination intensity was 2.15 cd s/m² that provided 8×10¹² photons/cm²/sec on the mounted eyecup preparations.

Recordings

An Ag-AgCl agar bridge electrode made of fine glass filled with 3 M KCl in 3% agar was set at both sides of the sample holder. The initial electrical signal generated by the mounted eye was received by a pre-amplifier (AI 417, Axon Instruments). These signals were further amplified with a D.C. main amplifier (CyberAmp380, Axon Instruments). The amplified signals were received by an AD/DA converter (Digidata 1200A interface, Axon instruments) and finally stored on a computer hard disc. The stored data were later processed using AxoScope 10.1 software (Axon Instruments, Inc.). The presented plots were prepared with Excel and Sigma Plot (version 2001) software. The signal gain was set at 5000.

Statistical Analysis

All the data shown are the mean values ± standard deviation (SD) of three to six experiments. The data was evaluated with Statistical Package for the Social Sciences (SPSS) software. Statistically significant *P*-values were set at *P* < 0.05.

Results and Discussion

Characterization of the NiONP

NiONP are biologically active nanomaterials with several biological and pharmacological properties in living cells, tissues, and animals [8, 9]. The morphological characterization of nanomaterials is necessary to ensure their use in biomedical applications [19, 20]. Therefore, the structure, shape, and size of synthesized NiONP were examined through XRD and TEM analysis. The XRD pattern of NiONP obtained after calcinations at 450°C has been displayed in Fig. 1. Strong and broad diffraction peaks were observed at 2θ (37.1, 42.2, and 63.1° matching to (111), (200), and (220) crystal planes, respectively. The peak positions matched with the peaks for NiONP reported earlier while the broadening of peaks provided a clear indication of smaller size of the particle [21]. These values

demonstrated the formation of cubic nickel oxide at the studied temperature. The average size of the nanoparticles was determined through X-ray diffraction line broadening using the Scherrer's equation:

$$L = K \cdot \lambda / B \cos \theta \quad (1)$$

L represents the particle size, *K* is the Scherrer constant, λ is the X-ray wavelength, θ is the diffraction angle of the peak, and *B* represents the Full-Width Half-Maximum (FWHM) of the peaks (in radians). The WFWM value calculated through Fityk software was 1.449 (°) while the average crystallite size was 57Å (5.7 nm). The XRD analysis also indicated that the NiONP have a polycrystalline structure (Fig. 1). The average particle size (5.7 nm) indicated that these nanoparticles are suitable for transport across the cell membrane. The purity of NiONP was confirmed by the absence of additional peaks in the XRD spectra.

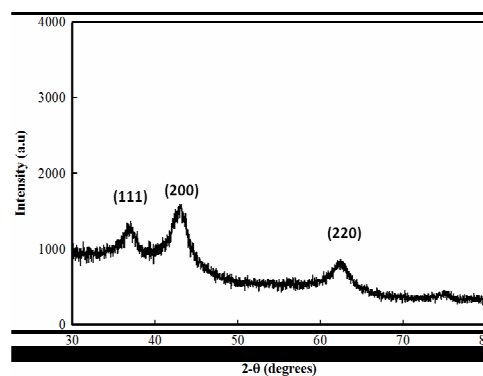


Fig. 1: X-ray diffraction pattern of the NiO nanoparticles. The absence of spurious diffraction indicates the crystallographic purity.

TEM images were recorded to measure the particle size distribution and also to confirm the dispersion of nanoparticles in ethanol. Particles were well separated and did not form agglomerates (Fig. 2). Furthermore, the TEM results showed that NiONP was predominantly round in shape. The diameters of 25 nanoparticles were measured and the particle size (diameter) and size distribution (mean diameter) were calculated. The results showed that it was ranged from 1.749 to 10.256 nm with the mean diameter of 7.143±2.078 nm (Fig. 3). The average particle size calculated from the TEM results (7.143) agreed with the XRD results (5.7 nm). The small size and non-agglomeration of the well-dispersed nanoparticles suggested the effectiveness of NiONP on the biological systems of the bullfrog eye.

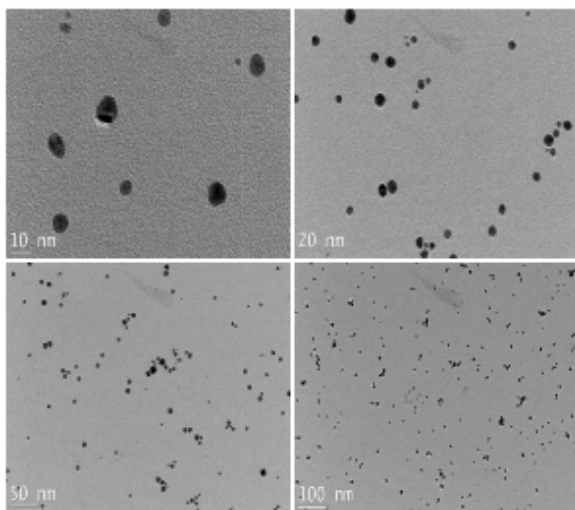


Fig. 2: TEM images of the NiO nanoparticles. The samples were prepared by drying (through solvent evaporation) the suspensions of NiO on glass plates.

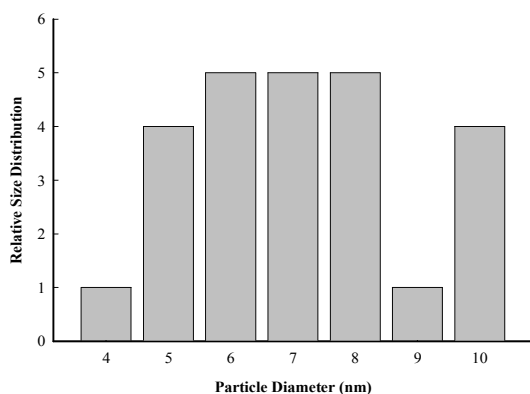


Fig. 3: Particle size distribution and average particles size of NiO nanoparticles calculated from the average size of 25 particles using ImageJ software.

Effects of NiONP on dark-adapted and light-adapted ERG b-wave amplitude

The ERG b-wave amplitudes was recorded under dark-adapted control ($n = 6$) and NiONP treatment conditions and compared. The NiONP treatment had a statistically significant improvement ($p < 0.05$) over dark-adapted ERG b-wave amplitudes throughout the entire range of light intensities (Fig.4).

To suppress the rod photoreceptors and determine the effects of NiONP on cone photoreceptors, a balanced background illumination (enough to suppress rod responses) was applied. The

NiONP produced statistically significant augmentation in ERG b-wave amplitude under background illumination (Fig. 5). The improvement in ERG b-wave amplitude was throughout the entire range of light intensities.

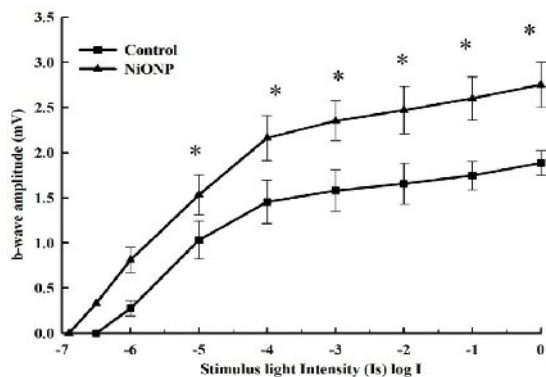


Fig. 4: Effects of NiONP on the dark-adapted ERG b-wave amplitude. The ERG was recorded from a bullfrog eyecup preparation using Ag-AgCl agar bridge electrodes. Total gain in the Axoscope was set at 5000. Data are shown as mean \pm SD from four independent experiments for each point. The significance was calculated compared to the control ($*p < 0.05$).

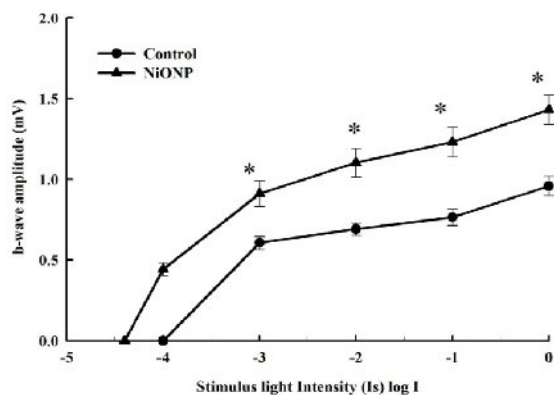


Fig. 5: Effects of NiONP in the presence of background illumination ($\log I = 0$). The ERG was recorded from a bullfrog eyecup preparation using Ag-AgCl agar bridge electrodes. Total gain in the Axoscope was set at 5000. Data are shown as mean \pm SD from four independent experiments for each point. The significance was calculated compared to the control ($*p < 0.05$).

The vertebrate retina has two types of light sensitive cells, which are known as rod and cone photoreceptors [22]. Rods work under dim light intensities and cones function under brighter light intensities [22]. These characteristics allow

researchers to differentiate the ERG responses obtained from the activities of rod and cone photoreceptors [22]. In this study, ERG responses generated under dim light intensities were considered as rod activities. The mixture of rod and cone responses were recorded under the mid-range of light intensities and the only cone-produced ERG was recorded under the brighter light intensities. NiONP improved the ERG b-wave amplitude both in dark-adapted and light-adapted status (Figure 4 and 5), which indicated that NiONP have the ability to improve the functions of both rods (Figure 4, dim intensity) and cones (Figure 5, under background illumination). Similarly, the mixture of rod and cone responses was also improved by the treatment with NiONP under a mid-range of intensities (Figure 4). The results provide clear evidence that NiONP improve the responses of both rod and cone photoreceptors.

Effects of NiONP on Visual Sensitivity

Any improvement in ERG sensitivity is an indication of enhancement in eyesight; thus, the positive effects of NiONP on ERG sensitivity were investigated. The dimmer flash intensity produced assessable ERG signals (10 μ V of b-wave selected as a threshold criterion) prior and following NiONP treatment (n = 4). NiONP treatment produced an average improvement of 0.4 log units of light intensity in ERG or visual sensitivity (Table-1).

Table-1: Threshold light intensity of ERG sensitivity for control and NiONP-treated groups (left). The duration (sec) needed for the recovery of threshold ERG after photo bleaching under different background illumination intensities (right). The time needed for ERG recovery was considered the duration of rhodopsin regeneration. The significance was calculated compared to the control (* $p < 0.05$).

Treatment	Threshold light intensity	Background Light Intensity (Ib) log I				
		-7 log I sec	-5 log I sec	-3 log I sec	-1 log I sec	0 log I sec
Control	-6.6 \pm 0.17 log I	<30	30	150	460	570
NiONP	-7.0 \pm 0.14 log I	<30	30	120	360	480

An enhanced activity of the retinal neural system improves the ERG b-wave amplitude [23]. NiONP seem to enhance retinal neurons activities through photoreceptors and other molecular receptors related with b-waves. Previous studies showed that besides photoreceptors, Muller cells as well as depolarizing bipolar cells are also closely associated with changes in ERG b-waves [13-17]. Therefore, NiONP may also improve the biological functions of Muller cells or depolarizing bipolar cells. Moreover, NiONP may enhance other receptors or cellular

pathways related to increments of ERG b-wave. NiONP treatment markedly improved visual sensitivity (Table-1). NiONP have beneficial effects on the outer retinal functions because these are directly associated with ERG [23].

Effects of NiONP on rhodopsin regeneration

To determine the effect of NiONP on rhodopsin regeneration, eyecup preparations were bleached under different background light intensities for 10 min. The time required for threshold recovery was recorded as the minimum duration required for the recovery of the threshold ERG, as it corresponds to the time required for rhodopsin regeneration. The duration required for rhodopsin regeneration (in sec) after photo-bleaching with different background light intensities was recorded and the NiONP treatment markedly shortened the time required for threshold ERG recovery (Table-1). This indicated that NiONP have accelerated the rhodopsin regeneration.

Rhodopsin is the photo-pigment that is abundantly found in retina and plays an important role in the visual cycle [24]. Upon light exposure, it undergoes phototransduction and rhodopsin is broken down into retinal and opsin [24]. After some time in the dark, the retinal and opsin proteins recombine through several intermediate steps and are converted to rhodopsin through rhodopsin regeneration [24]. However, diseased eyes require more time for rhodopsin regeneration compared to normal eyes [25]. In the current protocol, the time needed for the threshold ERG recovery after bleaching was considered as the time required for rhodopsin regeneration. Therefore, NiONP reduced the duration for rhodopsin regeneration (Table-1). The enhanced activity of alcohol dehydrogenase reduces the time required for rhodopsin regeneration [26, 27]. Thus, NiONP probably improve the function of alcohol dehydrogenase. In past, it was observed that the rate-limited supply of 11-*cis*-retinal from the retina pigment epithelium (RPE) to the outer side of the photoreceptors has direct effects on the rhodopsin cycle [27]. Therefore, NiONP may also enhance the rate-limited supply of 11-*cis*-retinal from the retina pigment epithelium (RPE) to the outer side of the photoreceptors.

Conclusion

Based on the results, NiONP treatment has beneficial effects on the neuronal and visual system of the vertebrate eye. In addition, NiONP also improve visual sensitivity and eyesight, and may be useful for treating delayed rhodopsin regeneration.

ERG techniques were used to evaluate the effect on NiONP on the visual system; therefore, advanced electrophysiological techniques (e.g., intracellular and patch clamp recordings) will be used to test NiONP in the future. Nevertheless, the current results give important scientific evidence that NiONP and other similar nanomaterials are useful for treating eye diseases.

Acknowledgements

This work was supported by the Kyungpook National University Research Fund, 2014.

References

1. F. Wahid, T. Khan, A. Shehzad, M. Ul-Islam and Y. Y. Kim, Interaction of Nanomaterials with Cells and Their Medical Applications, *J. Nanosci. Nanotechnol.*, **14**, 744 (2014).
2. F. Wahid, M. Ul-Islam, R. Khan, T. Khan, W. A. Khattak, K. H. Hwang, J. S. Park, S. C. Chang and Y. Y. Kim, Stimulatory Effects of Zinc Oxide Nanoparticles on Visual Sensitivity and Electroretinography b-waves in the Bullfrog Eye, *J. Biomed. Nanotechnol.*, **9**, 1408 (2013).
3. B. Sivakumar, R. G. Aswathy, R. Sreejith, Y. Nagaoka, S. Iwai, M. Suzuki, T. Fukuda, T. Hasumura, Y. Yoshida, T. Maekawa, and D. N. Sakthikuma, Bacterial Exopolysaccharide Based Magnetic Nanoparticles: A Versatile Nanotool for Cancer Cell Imaging, Targeted Drug Delivery and Synergistic Effect of Drug and Hyperthermia Mediated Cancer Therapy, *J. Biomed. Nanotechnol.*, **10**, 885 (2014).
4. H. Haase, A. Fahmi, and B. Mahltig, Impact of Silver Nanoparticles and Silver Ions on Innate Immune Cells, *J. Biomed. Nanotechnol.*, **10**, 1146 (2014).
5. S. K. Cho, K. Emoto, L. J. Su, X. Yang, T. W. Flaig, and W. Park, Functionalized Gold Nanorods for Thermal Ablation Treatment of Bladder Cancer, *J. Biomed. Nanotechnol.*, **10**, 1267 (2014).
6. M. S. Hassan, T. Amna, A. Mishra, S. I. Yun, H. C. Kim, H. Y. Kim, and M. S. Khil, Fabrication, Characterization and Antibacterial Effect of Novel Electrospun TiO₂ Nanorods on a Panel of Pathogenic Bacteria, *J. Biomed. Nanotechnol.*, **8**, 394 (2012).
7. S. Galdiero, A. Falanga, M. Vitiello, M. Cantisani, V. Marra, and M. Galdiero, Silver Nanoparticles as Potential Antiviral Agents, *Molecules.*, **16**, 8894 (2011).
8. Y. B. M. Mahaleh, S. K. Sadrnezhaad, and D. Hosseini, NiO Nanoparticles Synthesis by Chemical Precipitation and Effect of Applied Surfactant on Distribution of Particle Size, *J. Nanomater.*, **2008**, 1 (2008).
9. I. S. Lee, N. Lee, J. Park, B. H. Kim, Y. W. Yi, T. Kim, T. K. Kim, I. H. Lee, S. R. Paik, and T. Hyeon, Ni/NiO Core/Shell Nanoparticles for Selective Binding and Magnetic Separation of Histidine-tagged Proteins, *J. Am. Chem. Soc.*, **128**, 10658 (2006).
10. F. Wahid, H. Jung, T. Khan, K. H. Hwang, J. S. Park, S. C. Chang, M. A. Khan, and Y. Y. Kim, Effects of Rubus Coreanus Extract on Visual Processes in Bullfrog's Eye, *J. Ethnopharmacol.*, **138**, 333 (2011).
11. F. Wahid, H. Jung, T. Khan, K. H. Hwang, and Y. Y. Kim, Effects of Red Ginseng Extract on Visual Sensitivity and ERG b-wave of Bullfrog's Eye, *Planta Med.*, **76**, 426 (2010).
12. R. E. Carr, and I. M. Siegel, In *Analysis of the ERG Components, Visual Electrodiagnostic Testing: A Practical Guide for the Clinician*, Williams & Wilkins Press, Baltimore, p. 9 (1982).
13. K. T. Brown, The Electroretinogram: Its Components and Their Origins, *UCLA Forum Med. Sci.*, **8**, 319 (1969).
14. J. F. Hejtmancik, E. J. Fitzgibbon, and R. C. Caruso, In *Neuroscience in Medicine*, Humana Press, New York, p. 537 (2008).
15. R. A. Stockton, and M. M. Slaughter, B-wave of the Electroretinogram. A Reflection of ON Bipolar Cell Activity, *J. Gen. Physiol.*, **93**, 101 (1989).
16. R. Wen, and B. Oakley, K(+)-evoked Müller cell Depolarization Generates b-wave of Electroretinogram in Toad Retina, *Proc. Natl. Acad. Sci. U. S. A.* **87**, 2117 (1990).
17. R. H. Steinberg, R. Schmidt, and K. T. Brown, Intracellular Responses to Light from Cat Pigment Epithelium: Origin of the Electroretinogram c-wave, *Nature*, **227**, 728 (1970).
18. N. Dharmaraj, P. Prabu, S. Nagarajan, C. H. Kim, J. H. Park, and H. Y. Kim, Synthesis of Nickel Oxide Nanoparticles Using Nickel Acetate and Poly(vinyl acetate) Precursor, *Mater. Sci. Eng. B-Adv. Funct. Solid-State Mater.*, **128**, 111 (2006).
19. M. J. Akhtar, M. Ahamed, S. Kumar, M. M. Khan, J. Ahmad, and S. A. Alrokayan, Zinc Oxide Nanoparticles Selectively Induce Apoptosis in Human Cancer Cells Through Reactive Oxygen Species, *Int. J. Nanomed.*, **7**, 845 (2012).
20. R. Rajendran, C. Balakumar, H. A. M. Ahammed, S. Jayakumar, K. Vaideki, and E. M.

- Rajesh, Use of Zinc Oxide Nanoparticles for Production of Antimicrobial Textiles, *Int. J. Eng. Sci. Technol.*, **2**, 202 (2010).
21. H. Qiao, Z. Wei, H. Yang, L. Zhu, and X. Yan, Preparation and Characterization of NiO Nanoparticles by Anodic arc Plasma Method, *J. Nanomater.*, **2009**, 1 (2009).
 22. M. Biel, M. Seeliger, A. Pfeifer, K. Kohler, A. Gerstner, A. Ludwig, G. Jaissle, S. Fauser, E. Zrenner, and F. Hofmann, Selective Loss of Cone Function in Mice Lacking the Cyclic Nucleotide-gated Channel CNG3, *Proc. Natl. Acad. Sci. U. S. A.* **96**, 7553 (1999).
 23. L. Li, and J. E. Dowling, Effects of Dopamine Depletion on Visual Sensitivity of Zebrafish., *J. Neurosci.*, **20**, 1893 (2000).
 24. T. Maeda, J. P. V. Hooser, C. A. G. G. Driessen, S. Filipek, J. J. M. Janssen, and K. Palczewski, Evaluation of the Role of the Retinal G Protein-coupled Receptor (RGR) in the Vertebrate Retina *In-Vivo*, *J. Neurochem.*, **85**, 944 (2003).
 25. S. E. Ostroy, S. M. Frede, E. F. Wagner, C. G. Gaitatzes, and E. M. Janle, Decreased Rhodopsin Regeneration in Diabetic Mouse Eyes, *Invest. Ophthalmol. Vis. Sci.*, **35**, 3905 (1994).
 26. J. G. Dorea, and J. A. Olson, The Rate of Rhodopsin Regeneration in the Bleached Eyes of Zinc-deficient Rats in the Dark, *J. Nutr.*, **116**, 121 (1986).
 27. T. D. Lamb, and E. N. Pugh, Phototransduction, Dark Adaptation, and Rhodopsin Regeneration the Proctor Lecture, *Invest. Ophthalmol. Vis. Sci.*, **47**, 1538 (2006).